Spectroscopic Characterization of a Newly Isolated Cytochrome P450 from *Rhodococcus rhodochrous*

Lucia Banci,* Ivano Bertini,* Lindsay D. Eltis,‡§ and Roberta Pierattelli*
*Department of Chemistry, University of Florence, 50121 Firenze, Italy; ‡Gesellschaft für Biotechnologische Forschung, 3300 Braunschweig, Germany

ABSTRACT Cytochrome P450 (P450) from *Rhodococcus rhodochrous* have been characterized through circular dichroism and nuclear magnetic resonance (NMR) spectroscopy, both in the substrate-free and substrate-bound forms. The data are compared with those of $P450_{cam}$ and indicate a close similarity of the structure of the active site in the two proteins. The substrate-free species contains low-spin iron(III), while the 2-ethoxyphenol bound species contains high-spin iron(III). The substrate is in slow exchange on the NMR time scale. The binding of CN^- has been investigated and the final adduct characterized through NMR spectra.

Nuclear relaxation times of the isotropically shifted signals turn out to be shorter than in other heme proteins, both in the high- and in the low-spin species. This is the result of longer electron relaxation times in P450s than in peroxidases and metmyoglobin. This property, as well as the electron paramagnetic resonance (EPR) spectrum of the substrate-free form, are discussed in terms of the presence of the cysteine as the fifth ligand of the iron ion instead of a histidine as it occurs in peroxidases and myoglobin.

INTRODUCTION

Cytochrome P450s (P450 hereafter) constitute a class of ubiquitous monooxygenase hemeproteins of molecular weight 45,000 that catalyze the oxidation of a wide variety of compounds (1). Substrates for P450s include endogenous compounds such as steroids, fatty acids, and prostaglandins, as well as exogenous compounds such as pesticides, chemicals, and carcinogens (2). In the resting state, the heme iron is in the 3+ oxidation, low-spin state. During the proposed catalytic cycle several oxidation states of the iron occur (3), although the occurrence of some of these intermediates has yet to be conclusively established.

The binding of carbon monoxide to the reduced enzyme produces a split in the 420 nm Soret band, giving rise to bands at 364 and 450 nm (4, 5). The latter absorption distinguishes P450s from other heme proteins and so provides its name (6). It has been shown that this fingerprint band is characteristic of iron(II) porphyrins with a thiolate ligand *trans* to a CO ligand (7).

The first P450 purified was the camphor-hydroxylating enzyme from *Pseudomonas putida* ($P450_{cam}$) (8). The crystal structures of both the substrate-bound and substrate-free forms have been solved to high resolution (1.6 Å) (9, 10). The heme, a protoporphyrin IX, lies between two helices and is attached to the protein by a single cysteine residue, axially coordinated to the heme iron. The substrate-free enzyme structure shows a network of water molecules in the substrate binding site, one of which is close to the iron and could serve as the sixth axial ligand.

The catalytic cycle includes several steps (11). Upon substrate binding, the low-spin iron(III) species is transformed into a high-spin iron(III) species; uptake of one electron provides an iron(II) species that can bind an O_2 molecule. A second electron is then taken up, and heterolytic cleavage of the dioxygen molecule liberates a water molecule to form an active oxoiron intermediate with the iron in a Fe(V) state (or Fe(IV) with a cation radical delocalized on the heme ring), suggested to be the active hydroxylating agent (12).

Detailed structure-function studies of $P450_{cam}$ have led to the development of models for electron transfer, substrate binding, and oxygen activation in P450s (13, 14). In addition, through site-directed mutagenesis, Sligar et al. produced several mutants (13) on residues around the heme, which provided precious information on the enzymatic mechanism. For most of these mutants Poulos (14) performed the crystallographic characterization, which made it possible to correlate enzymatic behavior with structural variations.

P450s, both in the absence and in the presence of substrates or various ligand molecules, have been the object of extensive biophysical characterization performed with a number of techniques, including UV-visible (15, 16), magnetic circular dichroism (17–20), and EPR (21–25) spectroscopy as well as Mössbauer (26–28) and magnetic susceptibility measurements (29 and 30 and references therein). In contrast, nuclear magnetic resonance has been very rarely applied to P450. The lack of a more detailed characterization is due mainly to the intrinsic low resolution of the spectrum in conjunction with the large linewidth of the signals. A few reports are available that show the ^1H nuclear magnetic resonance (NMR) spectra of the substrate-free, substrate-bound, and cyanide-bound protein and of the reduced form (31–35).

Characterization of other P450s is critical in order to correlate their catalytic properties with their structural features. Several soluble P450 enzymes have been characterized from

Received for publication 11 January 1993 and in final form 29 March 1993.

Address reprint requests to Prof. Ivano Bertini, Department of Chemistry, University of Florence, Via Gino Capponi 7, 50121 Firenze, Italy, or Dr. Lindsay Eltis, Gesellschaft für Biotechnologische Forschung, Mascheroder Weg 1, 3300 Braunschweig, Germany.

§Biotechnology Laboratory, University of Britsh Columbia, Room 237, Wesbrook Building, 6175 University Boulevard, Vancouver, BC V6T 1Z3 Canada.

0006-3495/93/08/806/08 $2.00

microbial sources (36). Two such isozymes, $P450_{BM-3}$ and $P450_{terp}$, have been subject to preliminary X-ray crystallographic analysis (37).

We report here the spectroscopic characterization of a cytochrome P450 purified from *Rhodococcus rhodochrous* ($P450_{RR1}$). This isoenzyme is induced by *ortho*-substituted alkoxyphenols (38) and has been shown to catalyze the *o*-dealkylations of these compounds (39). Circular dichroism (CD), EPR, and ^1H NMR spectra are presented and are compared with those of the better characterized $P450_{cam}$. We will also discuss the NMR relaxation behavior of the iron ion in this class of proteins and compare it with that in other heme-containing proteins.

MATERIALS AND METHODS

$P450_{RR1}$ was purified from *R. rhodochrous* grown on 2-ethoxyphenol (2EP) as previously described (39). The P450 monooxygenase nature of the present protein was established on the basis of the reduced carbon monoxide UV-visible spectrum. Cytochrome concentrations were determined using the extinction coefficients published for $P450_{cam}$ (40). Substrate was removed from the protein by ion exchange chromatography as previously described (40).

CD spectra were recorded on a Jasco J-600 spectropolarimeter interfaced to a Commodore PC40-40 microcomputer. The concentration of cytochrome was 13.4 μM in 50 mM 3-[*N*-morpholino]propanesulfonic acid (MOPS), pH 7.0, at room temperature. Substrate was added to a concentration of 120 μM.

EPR measurements were carried out at 4.2 K on a Varian E9 spectrometer, working at 9.2 GHz. The concentration of the enzyme was 1.8–2.0 mM in 50 mM MOPS, pH 7.0.

^1H NMR spectra were recorded on Bruker MSL 200 and Bruker AMX 600 spectrometers operating at 200.13 and 600.14 MHz, respectively. The samples were 0.5–2.0 mM in 50 mM MOPS (pH 7.0) and 50 mM KCl in aqueous solution or in 0.1 M phosphate buffer (pH 7.0) and 50 mM KCl in D_2O solution. The NMR spectra are equal when recorded in the two buffers. 1D ^1H NMR spectra were performed with the SuperWEFT (41) pulse sequence, using various recycle times, or by presaturating the solvent signal during the relaxation delay. T_1 measurements were obtained by using either the saturation recovery method (42) (at 200 MHz) or the inversion recovery method (43) (at 600 MHz). The data were fitted by a nonlinear best fitting procedure, using the proper equations.

The ^1H NOE (nuclear Overhauser effect) experiments were performed at 600 MHz with the SuperWEFT pulse sequence for water signal suppression and were collected using the previous reported methodology (44). Several experiments with different recycle times and saturation pulse lengths were performed. For signals a and b a build-up of the NOE as a function of saturation time was carried out to estimate (*a*) T_1 of the signals dipolarly coupled with the irradiated signals, (*b*) their cross-relaxation, and hence (*c*) the proton-proton distance (45, 46). These experiments were recorded with a recycle time of 80 ms, varying the saturation time from 1 to 40 ms.

The data were analyzed with the following equation:

$$\eta_i(t) = \frac{\sigma_{ij}}{\rho_i}(1 - e^{-\rho_i t})$$

where σ_{ij} is the cross-relaxation rate between protons i and j, ρ_i is the selective relaxation rate of the proton on which the NOE effect is observed, and t is the saturation time.

RESULTS

Substrate-free $P450_{RR1}$

Fig. 1 shows the CD spectra of $P450_{RR1}$ in the absence of substrate. The spectrum of the substrate-free $P450_{RR1}$ is characterized by transitions at 340 and 418 nm in the Soret region, which are due to the π-π^* transitions of the porphyrin ring. In the visible region, two weak transitions at 541 and 683 nm are observed, together with a shoulder around 490 nm. This spectrum is almost identical to that of substrate-free $P450_{cam}$ (47) and indicates that the heme environments of these proteins are very similar.

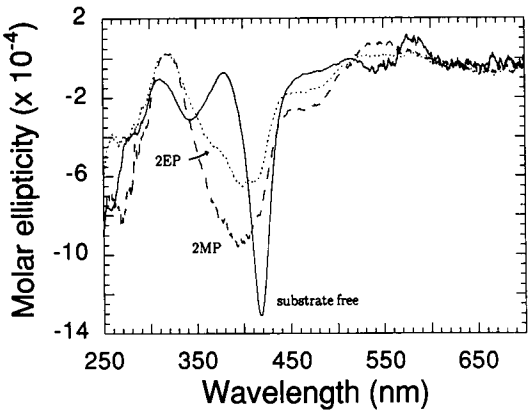

FIGURE 1 CD spectra of $P450_{RR1}$ in the absence of substrate (——), in the presence of 2EP (·····), and in the presence of 2MP (– – – –). The concentration of $P450_{RR1}$ was 13.4 μM in 50 mM MOPS, pH 7.0, at room temperature. Substrates were added to a concentration of 120 μM.

The 290 K, 200-MHz ^1H NMR spectrum of substrate-free $P450_{RR1}$ (Fig. 2) shows two broad signals at 23.3 ppm (signal a, linewidth 450 Hz) and 19.6 ppm (signal b, linewidth 400 Hz) of intensity 3, probably due to two methyl groups, plus a signal at 13.3 ppm (signal d) that disappears when the sample is exchanged in D_2O. The ^1H NMR spectrum recorded at 600 MHz in D_2O (Fig. 3) shows a few other resonances resolved from the diamagnetic envelope; besides a, b, and d, a very broad signal at 15.4 ppm (signal c) is observed. The T_1 at 600 MHz of a, b, and c signals are very short (3.6, 3.9 and 0.7 ms, respectively) and the linewidths are 500,

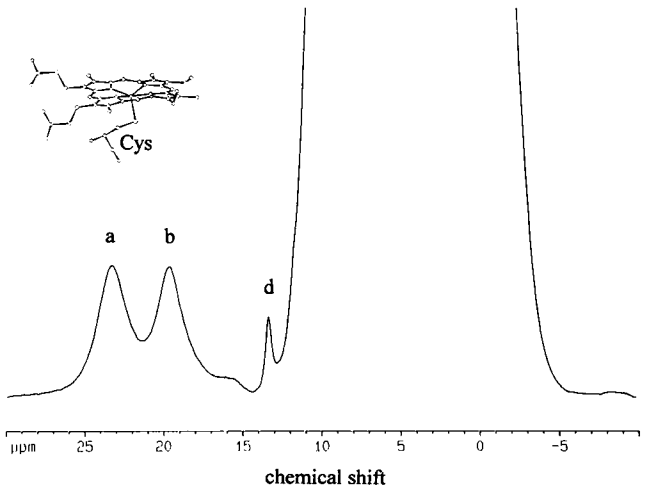

FIGURE 2 200 MHz ^1H NMR spectrum in H_2O of substrate-free $P450_{RR1}$. The concentration of $P450_{RR1}$ was 2.0 mM in 50 mM MOPS, pH 7.0, and 50 mM KCl. (*Inset*) Schematic representation of the heme-cys moiety.

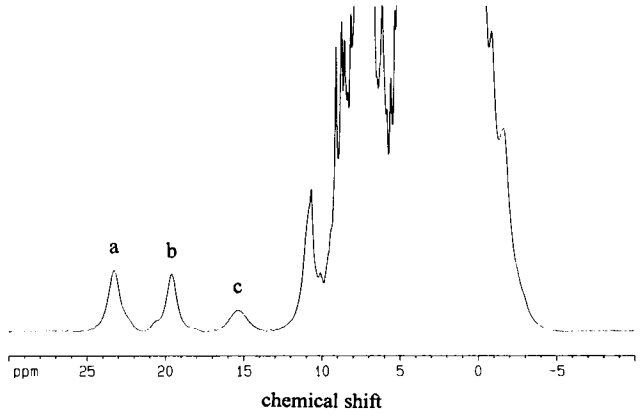

FIGURE 3 600 MHz ^{1}H NMR spectrum in D_2O of substrate-free $P450_{RR1}$. The concentration of $P450_{RR1}$ was 1.8 mM in 0.1 M phosphate buffer, pH 7.0, and 50 mM KCl. The labels indicate the same signals as in Fig. 2.

420 and 780 Hz. The shift of these signals shows a Curie-type behavior with temperature, indicating that the iron ion is in a single spin state. The shifts approximately extrapolate to the diamagnetic position at infinite temperature. These data indicate that the present system contains low spin iron(III), possibly six-coordinated by an axial water molecule, similar to $P450_{cam}$. Indeed, the ^{1}H NMR spectrum of $P450_{RR1}$ shows signals with shift and linewidth values very similar to those observed for $P450_{cam}$ (31).

The low-spin nature of the present protein is supported by the EPR spectrum at 4.2 K, the experimental g values (2.45, 2.26, and 1.92) of which are indicative of low-spin iron(III). This spectrum is also very similar to that reported for $P450_{cam}$ (47); both proteins are characterized by a relatively small magnetic anisotropy with respect to that of other low-spin heme proteins (48).

The NMR parameters of the substrate-free $P450_{RR1}$ spectrum are quite unusual as they are characterized by relatively small hyperfine shifts and by short nuclear relaxation times. While the former are consistent with the low-spin nature of the iron(III), even if smaller than those observed in other low-spin iron(III) heme proteins (49), short nuclear relaxation rates suggest that iron(III) is experiencing a long electron relaxation time. This is different from what is observed in other low-spin iron(III) systems (49), which are characterized by fast electron relaxation rates that cause relatively long T_1 and T_2 values of the protons sensing the metal ion. On the contrary, slow electron relaxation rates are present in high-spin iron(III) systems (49).

To further characterize the system, NOE experiments were performed. Saturation of signals a and b (Fig. 4*b–e*) with different saturation and recycle times provided NOEs on several signals in the diamagnetic envelope. From the build-up of these NOEs, proton-proton distances and T_1 values of these signals can be estimated; these are reported in Table 1. Inspection of Table 1 shows that the signals dipolarly coupled with the methyl signals are either characterized by T_1 values (all similar each other) about one order of magnitude longer

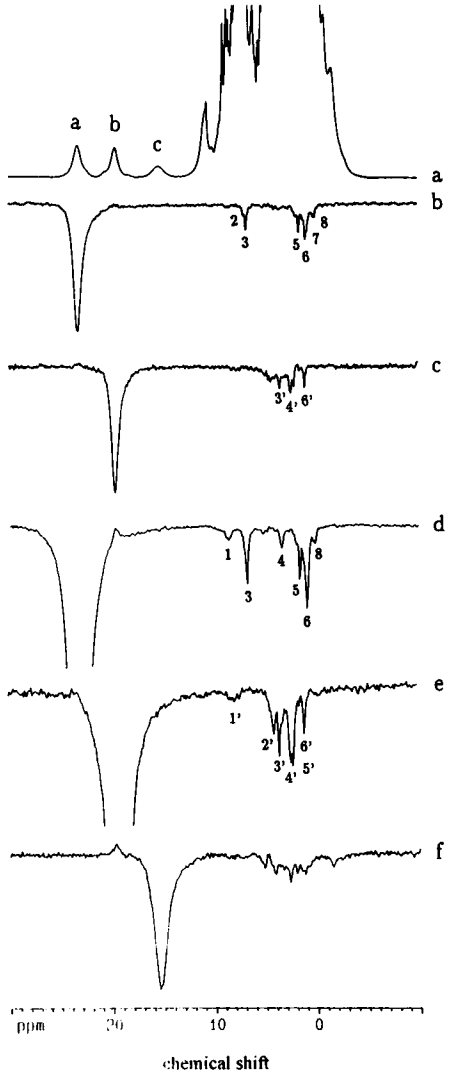

FIGURE 4 (*a*) 600 MHz spectra of substrate-free $P450_{RR1}$; (*b*) and (*c*) NOE difference spectra obtained upon saturation of signals a and b using a recycle time of 150 ms, and an irradiation time of 80 ms; (*d*), (*e*), and (*f*) NOE difference spectra obtained upon saturation of signals a, b, and c using a recycle delay of 30 ms and an irradiation time of 14 ms.

than those of the CH_3 signals, or by very short T_1s, in the range of those of methyl groups.

By saturation of a and b with fast repetition rates (Fig. 4, *d* and *e*) NOEs are detected and enhanced on broad signals 1 and 4 and 1′, respectively. The latter signals are characterized by short nuclear relaxation times, in the range of those measured for the CH_3 signals, thus indicating that signals 1, 4, and 1′ are due to protons at a distance from the iron ion similar to that for the CH_3. They might be due to the a protons of the heme side chains. At the present stage, however, we cannot perform a detailed assignment.

The T_1 values of the other signals dipolarly coupled with signals a and b are longer than those measured for the CH_3 groups, thus suggesting that the signals coupled with the latter groups are due to protons farther from the iron than the heme protons in α position. The properties of these signals suggest that some of them could be due to protons of the

TABLE 1—Chemical shifts and T_1 values (measured with an error of ±20%) of signals on which NOEs are observed by saturation of signals a and b of substrate-free $P450_{RR1}$ (see Fig. 4) and their calculated distances from the saturated signals

Signal	δ (ppm)	T_1 (ms)	d_{calc} (Å)
Signal a			
1	8.70	<10	
2	7.01	15	
3	6.76	14	2.7
4	3.61	<6	
5	1.63	16	2.8
6	0.87	14	2.5
7	0.79	14	
8	0.07	17	
Signal b			
1′	7.80	<5	
2′	4.40	18	
3′	3.51	13	2.5
4′	2.44	16	2.6
5′	2.12	18	2.7
6′	1.08	18	2.7

propionate or vinyl chains in β position; again, it is not possible to propose a definite assignment of the individual signals.

Due to the short T_1 and large linewidth, complete saturation of signal c cannot be achieved. It gives NOEs on a few signals in the diamagnetic envelope (Fig. 4*f*).

Nuclear Overhauser effect spectroscopy (NOESY) experiments, with various recycle and mixing times, were performed in an attempt to detect other dipolar connectivities. Several cross peaks are apparent but not enough in number to propose a sound assignment of the peaks.

$P450_{RR1}$ with substrate

Fig. 1 (*dashed lines*) reports the CD spectra of $P450_{RR1}$ in the presence of 2EP and 2-methoxyphenol (2MP). These compounds were discovered to be suitable substrates for the present P450 (38), as mentioned in the Introduction. The Soret Cotton effect of $P450_{RR1}$ is dominated by a negative absorption at 395 nm and a shoulder at 460 nm. These features are broader than the corresponding ones in the camphor-bound $P450_{cam}$. We attribute these differences to the aromatic nature of the substrate of $P450_{RR1}$. Myer (50) indicated that dichroic contributions originating from aromatic chromophores up to 12 Å away from the heme can influence the Soret Cotton effect of heme proteins. Indeed, replacement of Phe82 of iso-1-cytochrome *c*, a residue that sits in close proximity to the heme of this protein, with non-aromatic residues abolishes the negative Soret ellipticity of this protein (51), whereas replacement with tyrosine, another aromatic residue, does not perturb this negative Cotton effect. The crystal structure of substrate-bound $P450_{cam}$ (9) indicates that the camphor molecule binds to the protein in close proximity to the distal side of the heme chromophore. A substrate molecule bound to a similar location in $P450_{RR1}$ would be in a position to influence the symmetry of the heme group.

The small differences in the CD spectra of 2EP- and 2MP-bound $P450_{RR1}$ may be due to differences in how these substrates fit into the substrate-binding pocket and hence their position relative to the heme group.

The 290 K, 200-MHz ^1H NMR spectrum of $P450_{RR1}$ with 2EP (Fig. 5*A*) shows hyperfine shifted signals in the range of 80/10 ppm in the downfield region. Signals at 18.2 ppm and 13.9 ppm disappeared when the sample was exchanged in D_2O. There are no resolved signals in the upfield region. The downfield shifted signals experience very short T_1s and large linewidths. The shift values of the paramagnetic signals experience a Curie behavior with temperature, thus indicating the presence of a single spin species. The shift values extrapolate, at infinite temperature, approximately to the diamagnetic position, except for signal A. The shifts and T_1 values, the linewidths, and the temperature behavior indicate that the system essentially contains high-spin iron (III). This is consistent with what is observed in $P450_{cam}$ (Ref. 34 and I. Bertini et al., unpublished results). The ranges of the chemical shift of the resonances are quite similar to those of other high-spin iron(III) heme proteins, but the signals are broader and the T_1 shorter. The spectrum of $P450_{cam}$ in the presence of substrate (34) shows four signals of intensity 3 due to the methyl groups of the heme ring, two around 65 and two around 40 ppm, the two pairs being well separated each other (Fig. 5*B*). When the spectra of $P450_{RR1}$ and $P450_{cam}$ in the presence of substrate are compared, it appears that the composite signal B could be due to the overlap of the signals of two methyl groups of the heme moiety, while the other two methyl groups give rise to signals D and E.

In other heme proteins, with iron(III) in the high-spin form, the methyl groups experience a smaller spreading than that observed in $P450_{RR1}$ (52–57). The splitting of the methyl groups is essentially due to the heme plane anisotropy, determined by the axial ligand (58, 59). It could be that the

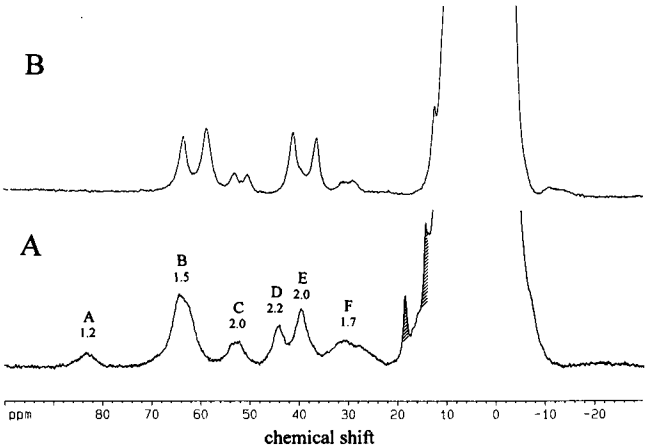

FIGURE 5 (*A*) 200 MHz ^1H NMR spectrum in H_2O of $P450_{RR1}$ with 2EP. The shaded signals correspond to exchangeable protons in D_2O. The concentration of $P450_{RR1}$ was 0.5 mM in 50 mM MOPS, pH 7.0, 50 mM KCl, and 1.0 mM 2EP. (*B*) 200 MHz ^1H NMR spectrum in H_2O of $P450_{cam}$. The concentration of $P450_{cam}$ was 0.5 mM in 50 mM phosphate buffer, pH 7.1, 50 mM KCl, and 1.0 mM camphor.

conformation of the axial cysteine group makes the heme plane asymmetric, thus making the methyl signals unequivalent.

The linewidths of all of these signals largely increase, from 200 MHz to 600 MHz, due to a large Curie contribution to the nuclear transverse relaxation time.

By partially eliminating the substrate through gel filtration, a sample containing both substrate-free and substrate-bound $P450_{RR1}$ was obtained. The spectrum of such samples shows both the signals of the high-spin form and those of the substrate-free derivative. This spectrum indicates that the substrate-free and -bound species are in slow exchange with respect to the NMR time scale. A lower limit of the exchange rate can be set around 5×10^4 s^{-1}.

$P450_{RR1}$ with CN^-

$P450_{RR1}$ has low affinity for cyanide, as reported for $P450_{cam}$ (25, 60). By the addition of CN^- to $P450_{RR1}$ the intensity of the signals present in the substrate-free spectra decreases and new resonances appear. At about 85 mM CN^-, the adduct is completely formed (Fig. 6).

The 292 K ^1H NMR spectrum of this adduct shows hyperfine shifted resolved signals at 26.0, 23.0, and 21.5 ppm, the first and the last being due to CH_3 groups. There are also resonances at −3.0, −3.8, and −4.5 ppm.

The K_d value was determined by fitting the decrease in intensity of the signals in the spectrum as a function of CN^- concentration. A value of 3.6 ± 0.4 mM was found (which is similar to what found for the $P450_{cam}$) (25, 60). The titration curve is shown in Fig. 6 (*inset*).

DISCUSSION

P450 proteins are characterized by longer electron relaxation times and shorter nuclear relaxation times than other hemoproteins with the same spin state (49).

The high-spin species has NMR chemical shifts of the order of those of peroxidases (53, 55–57), metmyoglobin (52), and Cyt c′ (61). However, in the latter systems 2D NOESY experiments, together with correlated spectroscopy (COSY) experiments, were successful and allowed a safe assignment of the heme protons and of other signals (61, 62). In the present case nuclear relaxation times did not allow us to perform useful experiments. The short nuclear relaxation times are the result of relatively long electron relaxation times for the iron ion in the present system. In turn, the electron relaxation times are found to depend on the magnitude of the zero field splitting (63): the larger the zero field splitting the shorter the electron relaxation times. This would indicate a relatively small zero field splitting value in the present system.

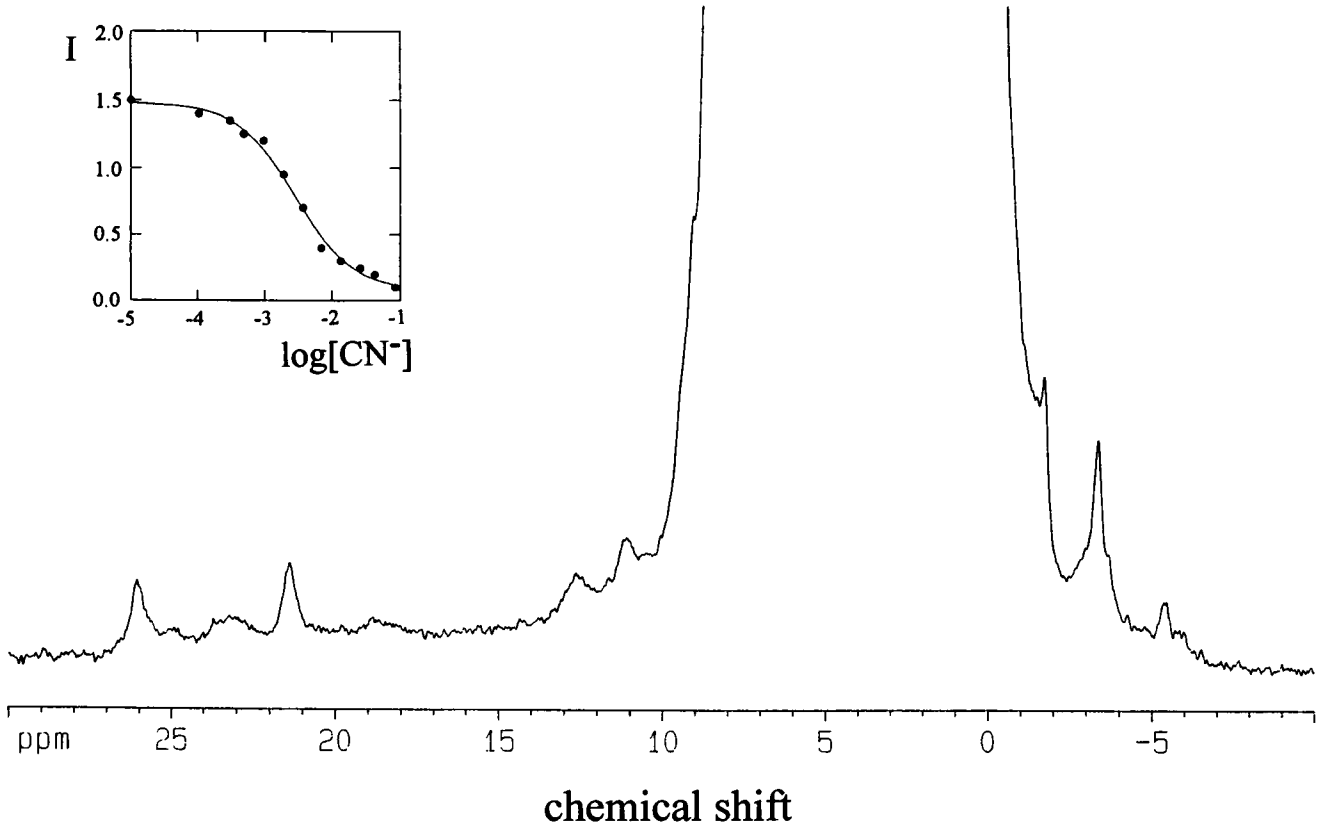

FIGURE 6 600 MHz ^1H NMR spectrum of $P450_{RR1}$ in the presence of 85 mM CN^-. (*Inset*) Titration curve. The concentration of $P450_{RR1}$ was 0.8 mM in 0.1 M phosphate buffer (pH 7.0) and 50 mM KCl in D_2O.

The low-spin species, with either water or CN^- as the sixth ligand, have also broad NMR lines with respect to the cyanide derivatives of peroxidases (57, 64–66) and metmyoglobin (52). Again, this is consistent with the data reported on $P450_{cam}$ and $P450_{cam}$-CN^- (31). Of course, the NMR lines are somewhat narrower than in the high-spin case. In six coordinated low-spin iron(III) compounds, there are three energy levels with $S = 1/2$, close in energy, which represent the ground state. The proximity of these levels is responsible for fast electron relaxation. If the splitting is within 1000 cm^{-1}, Orbach-type electron relaxation mechanisms are very efficient. This is what happens in the cyanide adducts of peroxidases (57, 64–66) and of metmyoglobin (52). The same electronic description in the latter systems accounts for the large deviation of the g values from 2. It seems that in P450s the splitting of the levels is significantly larger than 1000 cm^{-1}, and subsequently, electron relaxation is less efficient and g anisotropy is smaller. This could be due to the different nature of the axial ligand, i.e., cysteine in P450 versus histidine in peroxidases and metmyoglobin.

The cysteine ligand, with a sulfur donor atom, appears to be a strong donor ligand, stronger than histidine, which has a nitrogen. Indeed, in heme derivatives the axial pair of ligands Cys-H_2O provides low-spin species compared to the His-H_2O pair, which determines high-spin species, like in metmyoglobin. Cys-H_2O thus has the lowest axial donor strength capable of providing low-spin species. Consequently, among the low-spin species, it produces the largest anisotropy between axial and equatorial positions. The small g anisotropy is consistent with a large separation of the three $S = 1/2$ states.

The above picture is also consistent with the behavior of the high-spin form: being the cysteine ligand stronger than histidine, it determines the smaller zero field splitting of the $S = 5/2$ manifold. Consequently, the high-spin iron(III) ion in P450s has longer electron relaxation times than in metmyoglobin and therefore provides a shorter nuclear relaxation time and broader lines.

The spin density pattern on the heme ring could also be affected by the presence of a cysteine as an axial ligand. The spin density on the porphyrine ring in the low-spin iron(III) systems is believed to occur through p spin delocalization (59). The unpaired electron resides in the d_{xz}, d_{yz} level. In heme proteins having a histidine as an axial ligand the orientation of the imidazole ring splits the energy of the two ground state orbitals in such a way that the 3,8 and 1,5 methyls become pairwise nonequivalent. Even in the present case we observe only two methyl signals, which presumably are nonequivalent to the other two. The steric requirements that cause the cysteine to approach the iron in an unsymmetric way and make the sulfur p orbital to interact mainly with either the d_{xz} or the d_{xy} orbital are probably responsible for the splitting of the above levels and for the nonequivalence of the methyl groups (67, 68).

Finally, it is peculiar to note that CN^- binds the heme iron with low affinity, which is probably due to the presence in P450 of negatively charged residues in the proximity of the heme iron (60). From the NMR signal linewidths it appears that CN^- has also weaker donor strength than usual. Long electron relaxation rates and small g anisotropy have been also observed for the low-spin iron(III) in the CN^- adduct of chloroperoxidase, which has, like P450s, a cysteine as the fifth axial ligand (69).

The authors wish to thank Doctor Kenneth Timmis for his continuing interest in and support of the work and Professor Claudio Luchinat for discussion of the results.

REFERENCES

1. Wislocki, P. G., G. T. Miwa, and A. Y. Lu. 1980. Reaction catalyzed by the cytochrome P450 system. *In* Enzymatic Basis of Detoxification. W. B. Jacoby, editor. Academic Press, New York. 135–182.
2. Omura, T., R. Sato, D. Y. Cooper, O. Rosenthal, and R. W. Eastabrook. 1965. Function of cytochrome P450 of microsomes. *Fed. Proc.* 24: 1181–1189.
3. Dawson, J. H., and K. S. Eble. 1986. Cytochrome P450: heme iron coordination structure and mechanism of action. *In* Advances in Inorganic and Bioinorganic Mechanism. J. Sykes, editor. Academic Press, London. 2–64.
4. Hanson, L. K., W. A. Eaton, S. G. Sligar, I. C. Gunsalus, M. Gouterman, and C. R. Connell. 1976. Origin of the anomalous Soret spectra of carboxycytochrome P450. *J. Am. Chem. Soc.* 98:2672–2676.
5. Ullrich, V., H. H. Ruf, and P. Wende. 1977. The structure and mechanism of cytochrome P450. *Croat. Chem. Acta.* 49:213–222.
6. Omura, T., and R. Sato. 1964. CO-binding pigment of liver microsomes. Evidence for its hemoprotein nature, solubilization, purification and properties. *J. Biol. Chem.* 239:2370–2378.
7. Stern, J. O., and J. Peisach. 1974. Model compound study of the carbon monoxide adduct of cytochrome P450. *J. Biol. Chem.* 249:7495–7698.
8. Hedegaard, J., and I. C. Gunsalus. 1965. Mixed function oxidation. Induced methylene hydroxy-base in camphor oxidation. *J. Biol. Chem.* 240:4038–4043.
9. Poulos, T. L., B. C. Finzel, and A. J. Howard. 1987. High resolution crystal structure of cytochrome $P450_{cam}$. *J. Mol. Biol.* 195:687–700.
10. Poulos, T. L., B. C. Finzel, and A. J. Howard. 1986. Crystal structure of substrate-free *Pseudomonas putida* cytochrome P450. *Biochemistry.* 25:5314–5322.
11. Mansuy, D. 1987. Cytochrome P450 and synthetic models. *Pure Appl. Chem.* 59:759–770.
12. Atkins, W. M., and S. G. Sligar. 1988. Deuterim isotope effects in norcamphor metabolism by cytochrome $P450_{cam}$: kinetic evidence for two-electron reduction of a high-valent iron-oxo intermediate. *Biochemistry.* 27:1610–1616.
13. Sligar, S. G., D. Filipovic, and P. S. Stayton. 1991. Mutagenesis of cytochrome $P450_{cam}$ and b_5. *Methods Enzymol.* 206:31–49.
14. Poulos, T. L. 1991. Mutagenesis, modification, protein structure. *Methods Enzymol.* 206:11–30.
15. Gunsalus, I. C., and S. G. Sligar. 1978. Oxygen reduction by the P450 monoxygenase systems. *Adv. Enzymol.* 1–44.
16. Hanson, L. K., S. G. Sligar, and I. C. Gunsalus. 1977. Electronic structure of cytochrome P450. *Croat. Chem. Acta.* 49:237–250.
17. Dawson, J. H., P. M. Dolinger, J. R. Trudell, G. Barth, R. E. Linder, E. Bunnenberg, and C. Djerassi. 1974. Magnetic circular dichroism studies XXXV. A comparison of cytochromes P450 and P448. *Proc. Natl. Acad. Sci. USA.* 71:4594–4597.
18. Vickery, L., A. Salmon, and K. Sauer. 1975. Magnetic circular dichroism studies on microsomal aryl hydrocarbon hydroxylase: comparison with cytochrome b_5 and cytochrome $P450_{cam}$. *Biochim. Biophys. Acta.* 386:87–98.
19. Shimizu, T., T. Nozawa, M. Hatano, Y. Imai, and R. Sato. 1975. Magnetic circular dichroism studies of hepatic microsomal cytochrome P450. *Biochemistry.* 14:4172–4178.
20. Shimizu, T., T. Hzuca, H. Shimada, Y. Ishimura, T. Nozawa, and M. Hatano. 1981. Magnetic circular dichroism of cytochrome $P450_{cam}$.

Characterization of axial ligands of ferric and ferrous low-spin complexes. *Biochim. Biophys. Acta.* 670:341–354.

21. Hashimoto, Y., T. Yamano, and H. S. Mason. 1962. Electron spin resonance study of microsomal electron transport. *J. Biol. Chem.* 237: PC3843–PC3844.
22. Cammer, W., J. B. Schenkman, and R. W. Estabrook. 1966. Electron paramagnetic resonance measurements of substrate interaction with cytochrome P450. *Biochem. Biophys. Res. Commun.* 23:264–268.
23. Tsai, R. L., C. A. Yu, I. C. Gunsalus, J. Peisach, W. Blumberg, W. H. Orme-Johnson, and H. Beinert. 1970. Spin-state changes in cytochrome $P450_{cam}$ on binding of specific substrates. *Proc. Natl. Acad. Sci. USA.* 66:1157–1163.
24. Peisach, J., and W. E. Blumberg. 1970. Electron paramagnetic resonance study of the high and low spin forms of cytochrome P450 in liver and in liver microsomes from a methylcholanthrene-treated rabbit. *Proc. Natl. Acad. Sci. USA.* 67:172–179.
25. Sono, M., and J. H. Dawson. 1982. Formation of low spin complexes of ferric cytochrome $P450_{cam}$ with anionic ligands. *J. Biol. Chem.* 257: 5496–5502.
26. Sharrock, M., E. Münck, P. G. Debrunner, V. Marshall, J. D. Lipscomb, and I. C. Gunsalus. 1973. Mossbauer studies of cytochrome P450. *Biochemistry.* 12:258–265.
27. Munck, E., and P. M. Champion. 1975. Electronic structure of biomolecules. *Ann. N.Y. Acad. Sci.* 244:142–162.
28. Champion, P. M., J. D. Lipscomb, E. Munck, P. G. Debrunner, and I. C. Gunsalus. 1975. Mössbauer investigations of high spin ferrous heme proteins. I. Cytochrome P450. *Biochemistry.* 14:4151–4158.
29. Champion, P. M., E. Münck, P. G. Debrunner, T. H. Moss, J. D. Lipscomb, and I. C. Gunsalus. 1975. The magnetic susceptibility of reduced cytochrome $P450_{cam}$. *Biochim. Biophys. Acta.* 376:579–582.
30. Dawson, J. H., and M. Sono. 1987. Cytochrome P450 and chloroperoxidase: thiolate-ligated heme enzymes. Spectroscopic determination of their active site structure and mechanistic implications of thiolate ligation. *Chem. Rev.* 87:1255–1276.
31. Keller, R. M., K. J. Wüthrich, and P. G. Debrunner. 1972. Proton magnetic resonance reveals high-spin iron(II) in ferrous cytochrome $P450_{cam}$ from *Pseudomonas putida*. *Proc. Natl. Acad. Sci. USA.* 69: 2073–2075.
32. Griffin, B. W., and J. A. Peterson. 1975. *Pseudomonas putida* cytochrome P450. *J. Biol. Chem.* 250:6445–6451.
33. Philson, S. B., P. G. Debrunner, P. G. Schmidt, and I. C. Gunsalus. 1979. The effect of cytochrome $P450_{cam}$ on the NMR relaxation rate of water protons. *J. Biol. Chem.* 254:10173–10179.
34. Lukat, G. S., and H. M. Goff. 1990. A nuclear magnetic resonance study of axial ligation for the reduced states of cloroperoxidase, cytochrome $P450_{cam}$, and porphinatoiron(II) thiolate complexes. *Biochim. Biophys. Acta* 1037:351–359.
35. Sato, R., and T. Omura. 1978. NMR study of P450. *In* Cytochrome P450. Academic Press, New York. 127–131.
36. Sariaslani, F. S. 1991. Microbial cytochromes P450 and xenobiotic metabolism. *Adv. Appl. Microbiol.* 36:133–178.
37. Boddupalli, S. S., C. A. Haseman, K. G. Ravichandran, J.-Y. Lu, E. J. Goldsmith, J. Deisenhofer, and J. A. Peterson. 1992. Crystallization and preliminary X-ray diffraction analysis of $P450_{terp}$ and the hemoprotein domain of $P450_{BM-3}$, enzymes belonging to two distinct classes of the cytochrome P450 superfamily. *Proc. Natl. Acad. Sci. USA.* 89: 5567–5571.
38. Karlson, U., D. F. Dwyer, S. W. Hooper, E. R. B. Moore, K. N. Timmis, and L. D. Eltis. 1993. Two independently regulated cytochromes P450 in *Rhodococcus rhodochrous* that degrade 2-ethoxyphenol and 4-methoxybenzoate. *J. Bacteriol.* 175:1467–1474.
39. Eltis, L. D., U. Karlson, and K. N. Timmis. 1993. Purification and characterization of cytochrome $P450_{RR1}$ from *Rhodococcus rhodochrous*. *Eur. J. Biochem.* In press.
40. Gunsalus, I. C., and G. C. Wagner. 1978. Bacterial $P450_{cam}$ methylene monooxygenase components: cytochrome *m*, putidaredoxin and putidaredoxin reductase. *Methods Enzymol.* 52:166–188.
41. Inubushi, T., and E. D. Becker. 1983. Efficient detection of paramagnetically shifted NMR resonances by optimizing the WEFT pulse sequence. *J. Magn. Reson.* 51:128–133.
42. Markley, J. L., W. J. Horsley, and M. P. Klein. 1971. Spin-lattice relaxation measurement in slowly relaxing complex spectra. *J. Chem. Phys.* 55:3604–3605.
43. Vold, R. L., J. S. Waugh, M. P. Klein, and D. E. Phelps. 1968. Measurement of spin relaxation in complex system. *J. Chem. Phys.* 48: 3831–3832.
44. Banci, L., I. Bertini, C. Luchinat, M. Piccioli, A. Scozzafava, and P. Turano. 1989. ^1H NOE studies on dicopper(II) dicobalt(II) superoxide dismutase. *Inorg. Chem.* 28:4650–4656.
45. Johnson, R. D., S. Ramaprasad, and G. N. La Mar. 1983. A method of assigning functionally relevant amino acid residue resonances in paramagnetic hemoproteins using proton NOE measurements. *J. Am. Chem. Soc.* 105:7205–7206.
46. Banci, L., I. Bertini, C. Luchinat, and M. Piccioli. 1991. Frontiers in NMR of paramagnetic molecules: ^1H NOE and related experiments. *In* NMR and Biomolecular Structure. I. Bertini, H. Molinari, and N. Niccolai, editors. VCH, Weinheim. 31–60.
47. Peterson, J. A. 1971. Camphor binding by *Pseudomonas putida* cytochrome P450. *Arch. Biochem. Biophys.* 144:678–693.
48. Palmer, G. 1983. Electron paramagnetic resonance of hemoproteins. *In* Iron Porphyrins. A. B. P. Lever and H. B. Gray, editors. Addison Wesley, Reading. 43–88.
49. Bertini, I., and C. Luchinat. 1986. NMR of Paramagnetic Molecules in Biological Systems. Benjamin/Cummings, Menlo Park, CA.
50. Myer, Y. P. 1978. Circular dichroism spectroscopy of hemoproteins. *Methods Enzymol.* 54:249–284.
51. Rafferty, S. P., L. L. Pearce, P. D. Barker, J. Guy Guillemette, C. M. Kay, M. Smith, and A. G. Mauk. 1990. Electrochemical, kinetic and circular dichroic consequence of mutation at position 82 of Yeast iso-1-cytochrome *c*. *Biochemistry.* 29:9365–9369.
52. La Mar, G. N., D. L. Budd, K. M. Smith, and K. C. Langry. 1980. Nuclear magnetic resonance high spin ferric hemoproteins. Assignment of proton resonances in met-aquo myoglobins using deuterium-labeled hemes. *J. Am. Chem. Soc.* 102:1822–1827.
53. La Mar, G. N., J. S de Ropp, K. M. Smith, and K. C. Langry. 1980. Proton nuclear magnetic resonance study of the electronic and molecular structure of the heme crevice in horseradish peroxidase. *J. Biol. Chem.* 255:6646–6652.
54. Satterlee, J. D., J. E. Erman, G. N. La Mar, K. M. Smith, and K. C. Langry. 1983. Assignment of the hyperfine shifted resonances in high-spin forms of cytochrome *c* peroxidase by reconstitutions with deuterated hemins. *Biochim. Biophys. Acta.* 743:246–255.
55. de Ropp, J. S, G. N. La Mar, H. Wariishi, and M. H. Gold. 1991. NMR study of the active site of resting state and cynide-inhibited lignin peroxidase from *Phanerochaete chrysosporium*. Comparison with horseradish peroxidase. *J. Biol. Chem.* 266:15001–15008.
56. Banci, L., I. Bertini, P. Turano, M. Tien, and T. K. Kirk. 1991. Proton NMR investigation into the basis for the relatively high redox potential of lignin peroxidase. *Proc. Natl. Acad. Sci. USA.* 88:6956–6960.
57. Banci, L., I. Bertini, E. Pease, M. Tien, and P. Turano. 1992. ^1H NMR investigation of manganese peroxidases from *Phanerochaete chrysosporium* A comparison with other peroxidases. *Biochemistry.* 31:10009–10017.
58. La Mar, G. N., G. R. Eaton, R. H. Holm, and F. A. Walker. 1973. Proton magnetic resonance investigation of antiferromagnetic oxo-ligated ferric dimers and related high-spin monomeric ferric complexes. *J. Am. Chem. Soc.* 95:63–75.
59. La Mar, G. N., and F. A. Walker. 1979. Nuclear magnetic resonance of paramagnetic metalloporphyrins. *Porphyrins.* 4:61–157.
60. Lipscomb, J. D. 1980. Electron paramagnetic resonance detectable states of cytochrome $P450_{cam}$. *Biochemistry.* 19:3590–3599.
61. La Mar, G. N., J. T. Jackson, L. B. Dugad, M. A. Cusanovich, and R. G. Bartsch. 1990. Proton NMR study of the comparative electronic/magnetic properties and dynamics of the acid-alkaline transition in a series of ferricytochromes *c'*. *J. Biol. Chem.* 265:16173–16180.
62. de Ropp, J. S, and G. N. La Mar. 1991. 2D NMR assignment of hyperfine-shifted resonances in strongly paramagnetic metalloproteins: resting state horseradish peroxidase. *J. Am. Chem. Soc.* 113:4348–4350.
63. La Mar, G. N., and F. A. Walker. 1973. Proton nuclear magnetic resonace line widths and spin relaxation in paramagnetic metalloporphyrins of Cr(III), Mn(III), and Fe(III). *J. Am. Chem. Soc.* 95:6950–6956.
64. Satterlee, J. D., J. E. Erman, G. N. La Mar, K. M. Smith, and K. C.

Langry. 1983. Assignment of hyperfine-shifted resonances in low-spin forms of cytochrome *c* peroxidase by reconstructions with deuterated hemins. *J. Am. Chem. Soc.* 105:2099–2104.

65. Morishima, I., S. Ogawa, T. Inubushi, T. Yonezawa, and T. Iiuzuka. 1977. Nuclear magnetic resonance studies of hemoproteins. Acid-alkaline transition, ligand binding characteristics, and structure of the heme environments in horseradish peroxidase. *Biochemistry.* 16: 5109–5115.
66. de Ropp, J. S, G. N. La Mar, K. M. Smith, and K. C. Langry. 1984. Proton NMR studies of the electronic and molecular structure of ferric low-spin horseradish peroxidase complexes. *J. Am. Chem. Soc.* 106: 4438–4444.
67. Keller, R. M., and K. Wüthrich. 1978. Evolutionary change of the heme electronic structure: ferricytochrome *c*-551 from *Pseudomonas aeruginosa* and horse heart ferricytochrome *c*. *Biochem. Biophys. Res. Commun.* 83:1132–1139.
68. Senn, H., and K. Wüthrich. 1983. Individual proton NMR assignments for the heme groups and the axially bound amino acids and determination of the coordination geometry at the heme iron in a mixture of two isocytocromes. *Biochim. Biophys. Acta.* 743:69–81.
69. Dugad, L. B., X. Wang, C-C. Wang, G. S. Lukat, and H. M. Goff. 1992. Proton nuclear Overhauser effect study of the heme active site structure of chloroperoxidase. *Biochemistry.* 31:1651–1655.